

Supplemental material and methods.

Animal surgery.

Part of rats (n=40) were subjected to surgery. All surgical procedures were conducted under aseptic conditions according to most steps of the protocol previously published (Traissard et al., 2007). All rats sustained two surgical operations conducted in two steps, 7 days apart, the first one consisting in damaging the entorhinal cortex using N-methyl-D-aspartate, the second one in immunolesioning the cholinergic neurons of the medial septum using 192 IgG-saporin. As we focused on epigenetic regulation in the hippocampus, the cholinergic lesions were confined to the septal region by intraseptal injections of 192 IgG-saporin, whereas in the Traissard et al. study (2007), the lesions also altered a significant part of cholinergic neurons in the nucleus basalis and Purkinje neurons in the cerebellum, as 192 IgG-saporin was injected into the lateral ventricles. Histological verifications of lesion (placement/extent/specificity) are presented in supplemental material and methods. Two different groups of animal were performed: one group consisted of rats in basal conditions and corresponded to sham and lesioned home cage rats (n=10/group), the other group consisted of 3-day trained animals in the hidden platform version of the MWM (sham and lesion, n=10/group), about 3 weeks after the last surgery. ***Lesions of the entorhinal cortex (EC):*** For EC lesions, the rats were anaesthetised using an i.p. injection of pentobarbital (68.4 mg/kg; Ceva Santé Animale, Libourne, France) in saline. Lesions of the EC were performed with multiple injections of small amounts of N-Methyl-D-Aspartate (NMDA; 40 mM in PBS, pH 7.4) as previously described (Traissard et al., 2007). Briefly, NMDA was injected through a thin glass micropipette lowered into the brain at 6 sites per hemisphere, according to the following coordinates from Bregma (Paxinos and Watson, 1998): Site 1 ; A – 5.6 mm, L \pm 6.5 mm, V – 8.2 mm, Site 2; A – 6.3 mm, L \pm 6.2 mm, V – 8.2 mm, Site 3; A – 6.3 mm, L \pm 4.8 mm, V – 8.4 mm, Site 4; A – 7.0 mm, L \pm 5.1 mm, V – 8.0 mm, Site 5; A – 7.6 mm, L \pm 5.1 mm, V – 7.0 mm, Site 6; A – 8.3 mm, L \pm 4.6 mm, V – 5.0 mm. Injection volumes were 0.1 μ l in site 1, 0.2 μ l in sites 2 and 3, 0.3 μ l in sites 4 and 5, and 0.4 μ l in site 6. NMDA was injected at a flow rate of 0.2 μ l/min at each site. The micropipette was

left in place for 1-4 min before being retracted. Surgery in sham rats was similar except that no injection was made. **Lesions of the basal forebrain (BF) cholinergic neurons:** One week after EC lesions, rats were anaesthetized with i.p. injections of ketamine 100 mg/kg, 15 min after having received an i.p. injection of diazepam 3 mg/kg. Rats were subjected to injections into the medial septum and the vertical limb of the diagonal band of Broca of 192 IgG-saporin (at a concentration of 1.0 µg/µL of phosphate-buffered saline, Advanced Targeting System, San Diego, CA, USA, batch ##24-87) or of its vehicle (sham). Coordinates were (in mm from Bregma): A, +0.6; L, ± 0.2; V, -7.2 for the vertical limb of the diagonal band of Broca (0.1 µl/site, 2 sites) and V, -6.5 for the median septum (0.1 µl/site, 2 sites). The incisor bar was set at the level of the interaural line. At each site, after each injection, the needle was left *in situ* for 6 min before being retracted slowly.

Histological verifications in double lesion model

Preparation of tissue sections: After completion of the probe trial in the MWM, rats were decapitated, the brain removed and the dorsal hippocampus and the adjacent cortex were dissected separately on ice for biochemical analyses (see Methods section of the paper). The remaining brain was then post-fixed over 8 hrs with 4% paraformaldehyde (in 0.1 M PB; 4°C) and cryoprotected for 60 hr (at 4°C) in a 20% sucrose solution (in 0.1 M PB; 4°C). The brains were then snap-frozen in isopentane at -40°C and subsequently kept at -80°C until sectioning on a freezing microtome (Reichert Jung cryostat, Frigocut 2800) in coronal sections (40 µm thick).

Acetylcholinesterase histochemistry and cresyl violet staining: Sections were collected onto gelatine-coated slides and dried at room temperature. They were stained either with cresyl violet, according to Klüver and Barrera (1953) in order to identify the extent of EC lesion sites (which was confirmed on a few sections stained with anti-NeuN immunohistochemistry; see below), or for acetylcholinesterase (AChE) histochemistry according to Koelle (1954) with slight modifications in order to verify the extent of the cholinergic denervation in both the cortical mantle and the hippocampus. In the hippocampus, AChE activity is considered a reliable indicator of the degree of cholinergic innervation.

Quantification of AChE-positive staining: The extent of the cholinergic denervation was quantified by optical density (OD) measurements. Using a computer-assisted image analysis system (SAMBA Technologies, Meylan, France) coupled to a monochrome CCD digital Sony (Japan) video camera (Model XC 77CE) equipped with a 60 mm Nikon objective (Nikkor) and a Triplux extension tube, the mean OD was measured on digitalized images after precise delineation of each brain region of interest (i.e., the visual cortex, the auditory-perirhinal and entorhinal cortices, the amygdala, and the posterior hippocampus, in both its dorsal and ventral parts). For digitalization, sections were placed on a Kaiser Prolite 5000 light box (Kaiser Fototechnik, Buchen, Germany). Magnification from section to computer screen was 25. The mean OD considered as a “background” and subtracted from all measures before analysis was obtained from a value taken for each rat in the corpus callosum, where almost no AChE-positive reaction products could be identified. The experimenter performing the OD assessments was not aware of the rat’s treatment.

Anti-cholineacetyltransferase (ChAT), and anti-parvalbumine (Parv)

immunostaining: Anti-ChAT immunostaining was used to visualize the effects of 192 IgG-saporin on cholinergic neurons in the septum, diagonal band of Broca, nucleus basalis magnocellularis (NBM) and, as a control, for the selectivity of the toxin for basal forebrain cholinergic neurons, in the striatum. Anti-Parv immunostaining was used to control for possible effects of 192 IgG-saporin on GABAergic neurons in the septal region. For detailed immunohistological procedures see Traissard et al. (2007). Briefly, sections were rinsed three times during 10 min in PBSM (0.1 M PBS, pH 7.4, 0.02% merthiolate) before being soaked for 1 hr in 5% normal donkey serum (BioWest, Nuaille, France) in PBSM containing 0.5% Triton X-100. Then, the sections were transferred into the primary antibody solution (a goat polyclonal antibody directed against ChAT (1:1000, Chemicon International) or a mouse monoclonal antibody directed against Parv (1:4000, Sigma-Aldrich P3088)) for 18 hrs at room temperature. Then, all the sections preincubated with the anti-ChAT primary antibody were soaked for 1 hr in a buffer solution containing biotinylated donkey anti-goat antibody (1:500; Vector Laboratories International), and those preincubated with the anti-Parv primary antibody were soaked in a buffer solution containing biotinylated horse anti-mouse antibody (1:500; Vector

Laboratories International). After three PBSM washes, the sections were incubated for 45 min in a standard avidin-biotin-peroxidase complex (Vectastain Elite ABC, Vector Laboratories). The slices were then rinsed twice in PBSM and once in 0.6% Tris-buffer (pH= 7.6) and exposed to a solution of 0.0125% 3,3'-diaminobenzidine tetrahydrochloride (Sigma-Aldrich, Saint-Louis, MO) in Tris-buffer containing 0.0075% H₂O₂ until background staining saturation. Finally, after 3 PBSM rinses, the sections were mounted onto gelatine-coated slides, dried at room temperature, dehydrated and cover-slipped.

ChAT- and Parv-positive cell counting: To get an estimation of the lesion extent/selectivity induced by 192 IgG-saporin, anatomical landmarks were used to select, define, and standardize the location of counting frames of a set size in the medial septum (MS), the vertical limb of the diagonal band of Broca (vDBB), and the NBM as previously described (Traissard et al., 2007). Briefly, counting was made bilaterally on a particular section corresponding to an anteriority of Bregma +0.20 mm for counting in the MS and vDBB, and Bregma -1.4 mm for counting in the NBM. The number of ChAT- and Parv-positive neurons was determined separately in the MS, vDBB, and NBM (countings from left and right hemispheres added). For detailed anatomical localization of cell counting, see Traissard et al. (2007).

NeuN immunostaining: To complete the histological characterization of the EC lesion, a NeuN immunohistochemistry was realized in part of the sections. As for anti ChAT- and anti Parv-immunostaining (see upper paragraph), the sections were rinsed three times during 10 min in PBSM before being soaked for 1 hr in 5% normal donkey serum in PBSM containing 0.5 % Triton X-100. The sections were subsequently transferred into the primary antibody solution, a mouse NeuN antibody (1:2000, Chemicon International, ref MAB377) for 18 hr at room temperature. Then, the sections were soaked in a buffer solution containing biotinylated anti-mouse horse antibody (1:500; Vector Laboratories International). The next steps were exactly the same as for the Parv- and ChAT immunohistochemistry procedure described above.

References

Traissard N, Herbeaux K, Cosquer B, Jeltsch H, Ferry B, Galani R, Pernon A, Majchrzak

M, Cassel JC (2007) Combined damage to entorhinal cortex and cholinergic basal forebrain neurons, two early neurodegenerative features accompanying Alzheimer's disease: effects on locomotor activity and memory functions in rats. *Neuropsychopharmacology* 32:851-871.

Klüver H, Barrera E (1953). A method for the combined staining of cells and fibers in the nervous system. *J Neuropathol Exp Neurol* 12:400–403.

Koelle GB (1954). The histochemical localization of cholinesterases in the central nervous system of the rat. *J Comp Neurol* 100:211–235.

Immunolabeling of rat hippocampic neurons.

Five rats of each condition (VPf and HPf) were deeply anesthetized with an ip injection of pentobarbital (200 mg/kg) and perfused transcardially with 150 ml of ice-cold paraformaldehyde (4% in 0.1M PB, 4°C). Brains were rapidly removed from the skull and post-fixed for 2 hr in the same fixative at +4°C. Brains were then frozen and The dorsal hippocampus region (from -2.30 to -4.16 mm from Bregma, according to Paxinos and Watson, 1998) was cut into 20 µm thick slices with a cryostat. Permeabilization was performed with PBS1X/Triton 2% during 15 min. Unspecific labelling was blocked with PBS1X/Triton 0,1%/Horse serum 5% during 30 min at 37°C. Slices were incubated overnight with polyclonal anti CBP (1/100) antibody (sc-369, Santa Cruz biotechnology, CA, USA) or polyclonal anti acetylated-H2B K12K15 (1/250) antibody (ab1759, Abcam, Cambridge, UK) or MAP2 antibody (M4403, SIGMA, St Louis, MO) in PBS1X/Triton 0,1%/Horse serum 5%. Secondary antibodies were a alexa Fluor 488 goat anti rabbit IgG (H+L) and alexa Fluor 594 donkey anti mouse IgG (H+L) (Molecular Probes, CA, USA). Slices were incubated with the Hoechst dye 33342 (1 mg/ml ; 5 min) and mounted in mowiol for observation. Acquisitions were performed with a Nikon Digital Camera DXM 1200 (NIS-Elements F 2.20).

Primers for PCR amplifications.

Gene name	Sequences	Amplicon size
BDNF_EIV	L: 5'-GAG-CAG-CTG-CCT-TGA-TGT-TT-3' R: 5'-GTG-GAC-GTT-TGC-TTC-TTT-CA-3'	148
Zif268	L: 5'-TAC-GAG-CAC-CTG-ACC-ACA-GA-3' R: 5'-GGG-TAG-TTT-GGC-TGG-GAT-AAC-3'	91
cFos	L: 5'-GGG-ACA-GCC-TTT-CCT-ACT-ACC-3' R: 5'-GAT-CTG-CGC-AAA-AGT-CCT-GT-3'	87
Fos B	L: 5'-TGC-AGC-TAA-ATG-CAG-AAA-CC-3' R: 5'-CTC-TTC-GAG-CTG-ATC-CGT-TT-3'	73
CBP	L: 5'-AAG-AAT-ATG-GCT-CCG-ATT-GC-3' R: 5'-TGA-GGA-TCT-CAT-GGT-AAA-CAG-C-3'	120
P300	L: 5'-AAG-CAC-CAG-TGT-CTC-AAG-CA-3' R: 5'-CCC-TGG-AGG-CAT-TAT-AGG-AGA-3'	71
PCAF	L: 5'-GCT-TTA-CAG-CAC-GCT-CAA-GA-3' R: 5'-GTT-CCA-TGA-AGG-GCC-AAG-3'	71
Tip60	L: 5'-ACA-ATG-TGG-CCT-GCA-TCT-T-3' R: 5'-CTT-CTA-CTT-TCG-AGA-GTT-CAT-AGC-TG-3'	96
RNA PolIII	L: 5'-TTC-GGC-TCA-GTG-GAG-AGG-3' R: 5'-GCT-CCC-ACC-ATT-TCT-CCA-G-3'	94
18S	L: 5'-TTC-CTT-GGA-TGT-GGT-AGC-CG-3' R: 5'-CGT-CTG-CCC-TAT-CAA-CTT-TCG-3'	120

Optical density and area measurements.

Quantification of the relative optical densities (OD) of neuronal CBP immunoreactivity was examined in 6 to 8 coronal 40 μ m-thick sections of the dorsal hippocampus per rat by an experimenter blind to the experimental conditions. Stained sections were observed using a Leica DM5500B light microscope (x10 objective lens) and digitalized using a video camera (Optronics Microfire) online with an image analyzer (Explora Nova, La Rochelle, France). OD measurements were performed using a densitometry software program (Mercator) on two areas of the dorsal hippocampus: the CA1 pyramidal cell layer (over about 1.6 mm in the mediolateral plan) and the whole dentate gyrus granular (DG) layer. The same intensity of light in the microscope as well as the same parameters in the digital camera were used for all sections. After delimitation of the

region of interest, the OD measurements of the neuronal layer were performed by selecting a threshold value that keeps all labeled immunopositive elements but no background. The ODs measured in the stratum radiatum layer, and thus a region devoid of cell bodies, the OD of the auditory cortex was also measured as a control to verify the absence of increase of CBP levels during memory formation in this area. Indeed, the auditory cortex present on the same sections along with the dorsal hippocampus, appeared a good candidate as it seemed reasonable to expect minimal effects of learning in this area; its sound or noise-related activation should be comparable in HPf and VPf rats. was subtracted from the ODs corresponding to the CBP immunoreactivity in the defined areas of interest. The statistical analyses were performed using a two-way ANOVA considering Platform visibility (VPf, HPf) and Region (CA1, DG) as factors. Post hoc comparisons used the Newman–Keuls multiple range test. Values of $p < 0.05$ were considered significant.

Primers for PCR amplifications after chromatin immunoprecipitation.

Rat *Bdnf-pIV* primers have been described in Ou and Gean (2007). *Beta-actin* served as positive control and primers were from ChIP-IT TM Control Kit – Rat (53012, Active Motif). The different primers for rat *cFos*, *FosB* and *Zif268* proximal promoter regions PCR amplification were designed as follow (Str.: strand; Chr.: chromosome):

Gene name	Gene ID / NCBI Ref Seq	Str./Chr.	Primer sequence	Position
cFos	314322 / NC_005105.2	(+) / 6	L : 5'-AACCATCCCCGAAATCCTAC-3' R : 5'-AGCGGAACAGAGAAACTGGA-3'	109,558,890 109,559,074
<i>FosB</i>	308411 / NC_005100.2	(-) / 1	L : 5'-GTGAGGGGACTGCATCCTTA-3' R : 5'-GCTGGTGAAAAAGAGCAAGG-3'	78,674,443 78,674,338
<i>Zif268</i>	24330 / NC_005117.2	(+) / 18	L : 5'-ATGGGAGGTCTTCACGTAC-3' R : 5'-CGAATCGGCCTCTATTTCAA-3'	27,343,404 27,343,543
<i>cbp</i>	24330 / NM_133381.2	(+) / 10	L : 5'-GTGAAGATGGCCGAGAACTT -3' R : 5'-CAACCTCACCTGTGCTGTCA -3'	11,598,546 11,599,226

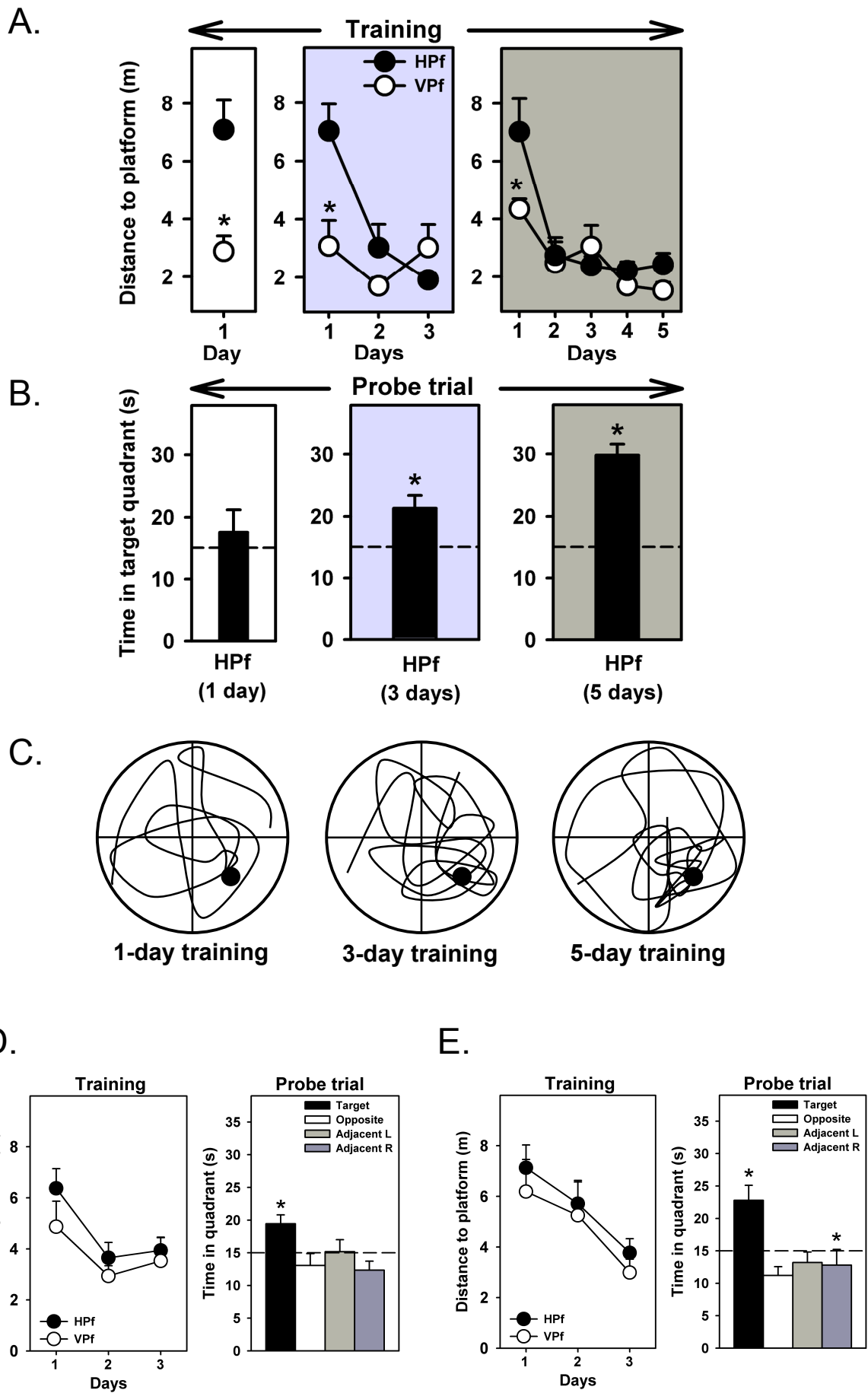


Figure S1

Cerebellum

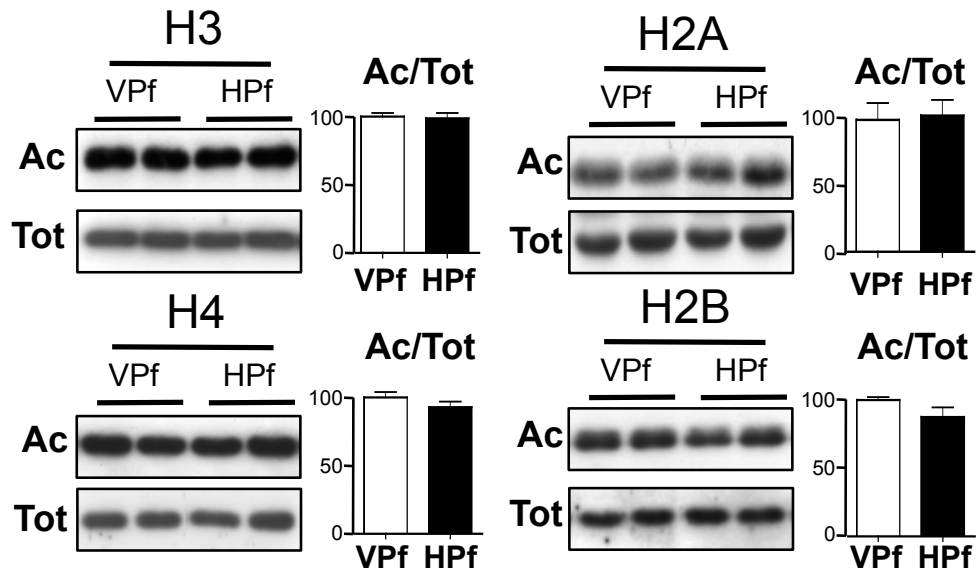


Figure S2

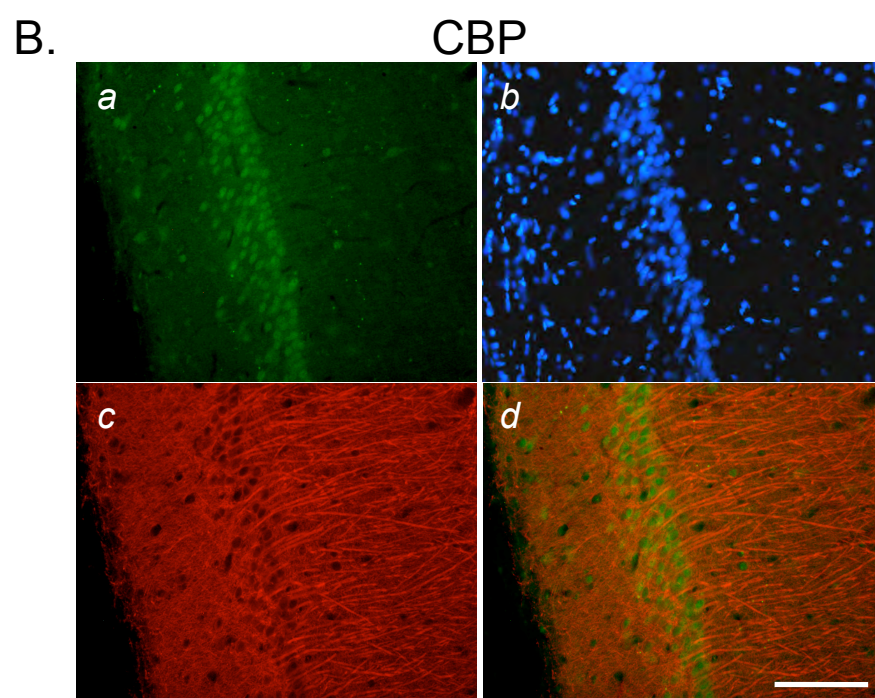
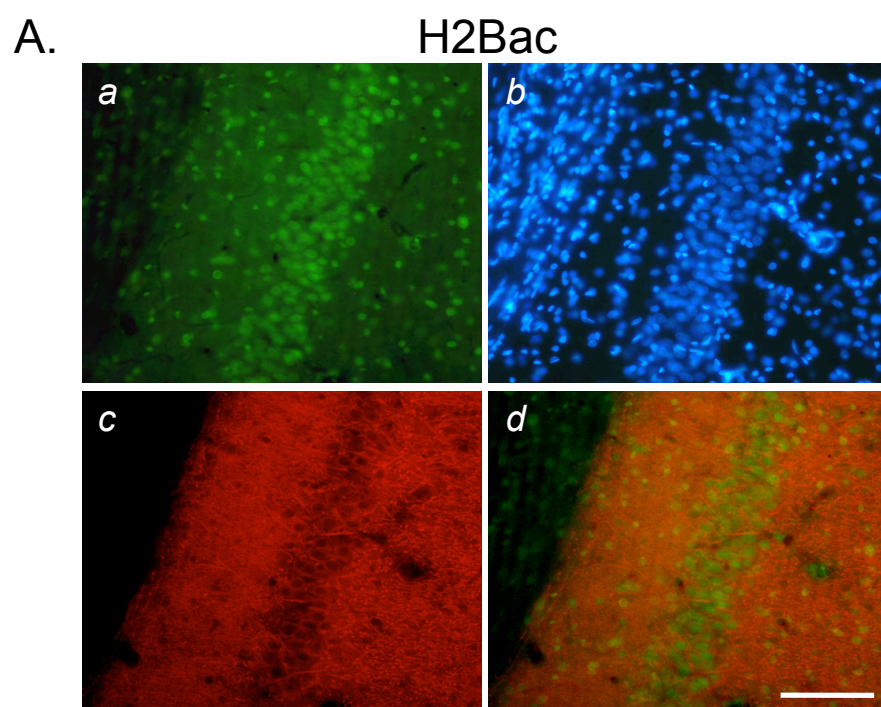
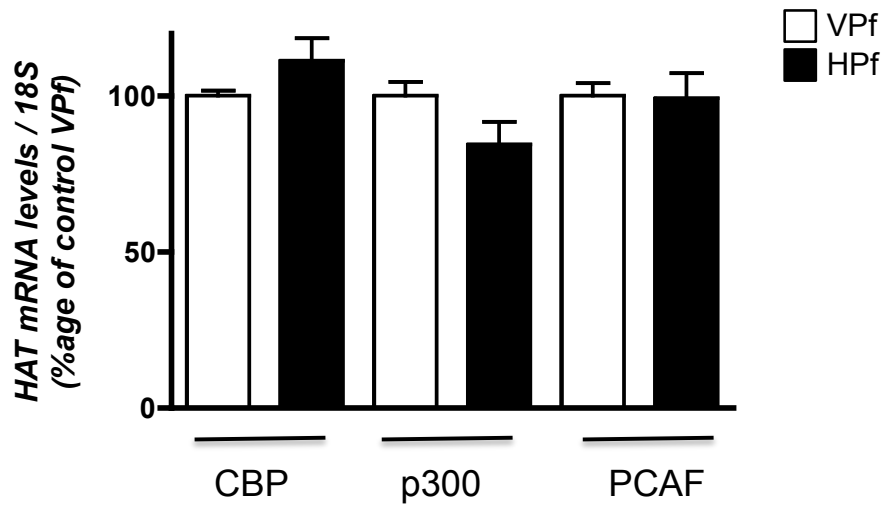


Figure S3

A.



B.

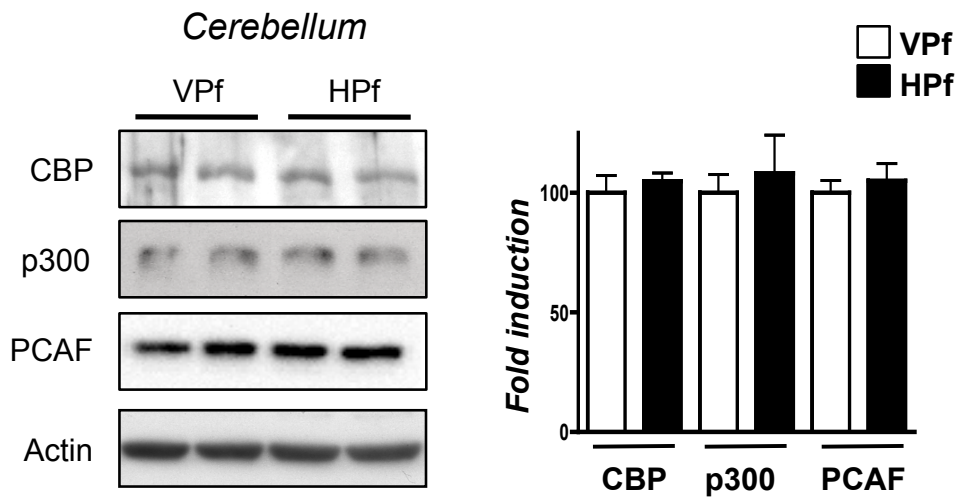
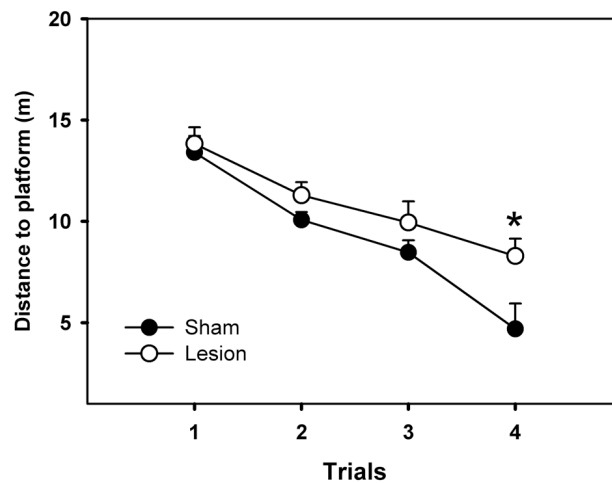


Figure S4

A.

Brain Region	Sham	Lesion
OD of AChE staining (arbitrary units)		
Visual cortex (V1, V2)	140 ± 16	147 ± 16
Auditory and perirhinal cortices	243 ± 30	327 ± 40
Entorhinal cortex	460 ± 68	429 ± 66
Amygdala	948 ± 106	847 ± 156
Posterior hippocampus, dorsal	1030 ± 83	556 ± 151 * (-47%)
Posterior hippocampus, ventral	714 ± 97	378 ± 89 * (-47%)
ChAT-positive neurons		
Medial septum	41.5 ± 5.0	6.3 ± 1.3 * (-85%)
Diagonal band of Broca (vertical limb)	19.1 ± 0.8	3.3 ± 1.6 * (-83%)
Nucleus basalis magnocellularis	129.2 ± 21.4	89.0 ± 9.2 * (-31%)
Parv-positive neurons		
Medial septum	21.5 ± 2.4	14.5 ± 4.3
Diagonal band of Broca (vertical limb)	33.5 ± 2.5	17.4 ± 4.8 * (-48%)
Nucleus basalis magnocellularis	33.0 ± 3.3	26.3 ± 3.0

B.



C.

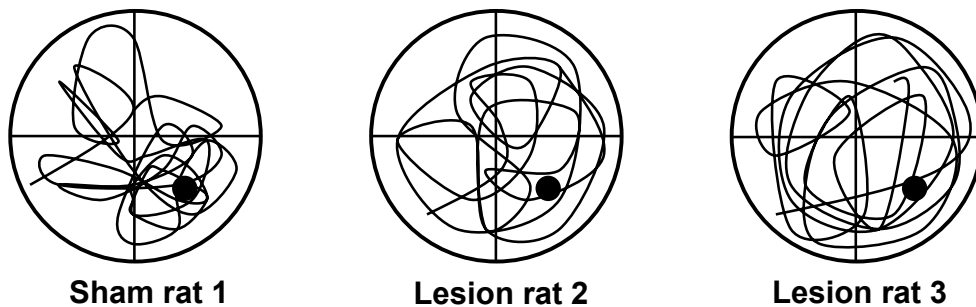


Figure S5

Cerebellum

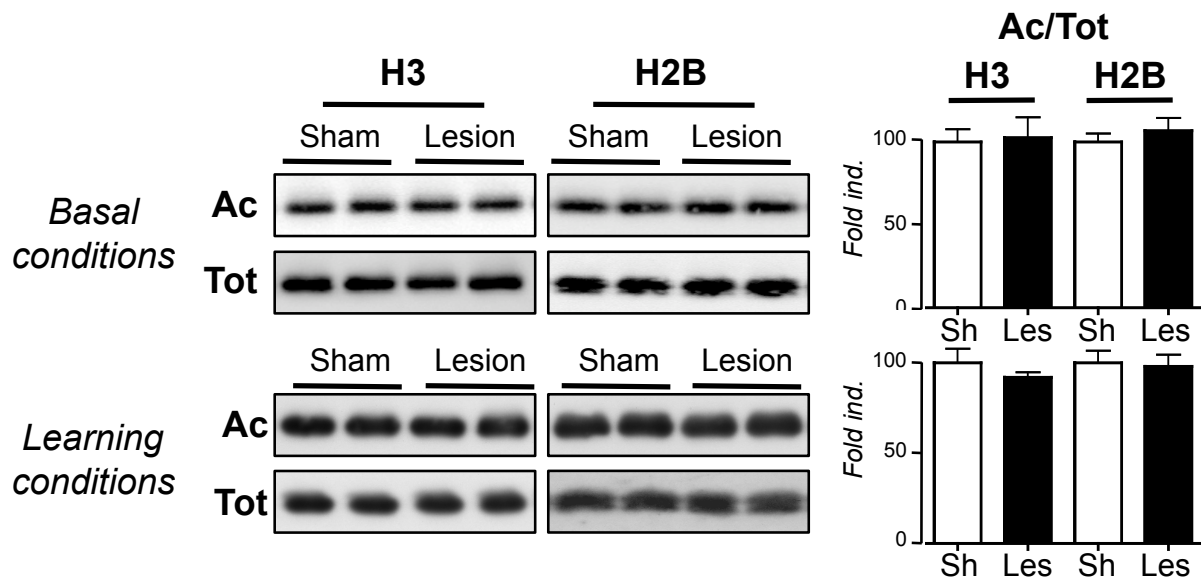


Figure S6

Supplemental legends:

Supplemental figure 1: Behavior analysis of rats during the time course of

spatial memory formation in the Morris water maze. Water maze performance of two groups of rats ($n = 15$ in each group at the start of training) over a 5-day training period. Rats were trained for 1 (A, left), 3 (A, middle) or 5 days (A, right), for part of them with a visible platform (VPf), for the other part with a hidden one (HPf). The VPf group had to swim to a platform whose location was changed from trial to trial. The HPf group had to swim to a platform that was kept at the same location for all trials.

(A) Acquisition data are expressed as mean (\pm SEM) distances to reach the platform on each day. HPf rats showed a marked improvement between day 1 and day 2, and reached an almost maximal performance on day 3. * $p < 0.01$, significantly different from HPf group. In the control group, whatever the number of subsequent training days (i.e., no, 2 or 4), VPf rats showed an average distance that was significantly shorter ($p < 0.01$ in the 1-day, 3-day and 5-day groups) as compared to that found in HPf rats. Over 5 days, performance did further improve (i.e. distance to reach the platform did further decrease) on subsequent days, especially after day 3, indicating that the control rats were able to gain in detection efficacy and/or swim efficiency (day 5 vs. day 1, $p < 0.05$). **(B)** At days 1, 3 and 5, randomly chosen rats in the HPf group were subjected to a probe trial (60 s), performed 1hr after the last training. VPf rats were only given a one-trial swim to visible platform trial. Mean time in the target quadrant (\pm SEM) showed performance which improved as a function of the number of training days: after 3 or 5 days of acquisition, rats showed a performance that was significantly above chance (i.e., 15 s) and which accounted for the retention of the platform location. * $p < 0.05$, significantly above chance (dashed line). **(C)** Typical swim tracks obtained after each training day (as noted) for rats navigating to the hidden platform. The former location of the platform is indicated by the black-filled circle in the south-east quadrant. **(D)** Water maze performance in rats ($n=8$ /group) trained over 3 consecutive days (4 trials/day) and used for the ChiP and nuclear extract experiments. See legend of Figure 1A and Method section for detailed behavioral protocol. Left: Acquisition data are expressed as mean (\pm SEM) distance to reach the platform. In both groups a significant decrease of the distance to reach the platform over days was observed (two-way ANOVA: $F_{(2,28)} = 8.56$, $p < 0.005$). Right: Probe trial performance in the HPf rats expressed as the mean search time in

each of the four quadrants (\pm SEM). Performance was above chance level (i.e., 15 s) only in the target quadrant ($t_7 = 3.23$, $p < 0.05$), whereas time in the three other quadrants was at chance level ($t_7 = -1.07$ or -1.92 or 0.09 , $p > 0.05$ for the opposite, adjacent left and right quadrants, respectively). * $p < 0.05$, significantly different from chance. **(E)** Water maze performance in rats ($n=5/\text{group}$) trained over 3 consecutive days (4 trials/day) and used for the Immunohistochemistry experiment. See legend of Figure 1A and Method section for detailed behavioral protocol. Left: Acquisition data are expressed as mean (\pm SEM) distance to reach the platform. In both groups a significant decrease of the distance to reach the platform over days was observed (two-way ANOVA: $F_{(2,16)} = 4.55$, $p < 0.05$). Right: Probe trial performance in the HPf rats expressed as the mean search time in each of the four quadrants (\pm SEM). Performance was above chance level (i.e., 15 s) only in the target quadrant ($t_4 = 3.89$, $p < 0.05$), whereas time in the three other quadrants was either at chance level ($t_4 = -0.91$ or -1.11 , $p > 0.05$ for right and left quadrants, respectively) or significantly underneath ($t_4 = -3.39$, $p < 0.05$ for opposite quadrant). * $p < 0.05$, significantly different from chance.

Supplemental figure 2: Measurement of histone acetylation levels in the cerebellum during the formation of a spatial memory. Acetylated (Ac) and total (Tot) histone levels were measured by Western blot analyses for each histone core in histone extracts obtained from the cerebellum of the same rats used in figure 1B (3-day trained rats; HPf *versus* VPf; $n = 7$ per group). Lysine acetylations measured were H3K9K14, H4K12, H2AK9 and H2BK5K10K15K20. Typical western blots are represented in duplicates. Quantified results are represented as fold induction of the Ac/Tot ratio for each histone, the ratio obtained in the control condition being arbitrarily set at 100%. A student *t*-test revealed no significant change between both groups (VPf *versus* HPf) for each core histone.

Supplemental figure 3: Acetylated-H2B and CBP/MAP2 immunofluorolabelings in hippocampic neurons. **(A)** Acetylated-H2B/MAP2 co-labeling was performed by immunofluorescence on rat brain sections. Representative photographs of the CA1 region are shown for acetylated H2B (a), MAP2 (c) and merged (d) labelings. The total number of cells is visualized by Hoechst staining of nuclei (b). H2B is acetylated in most of the cells. **(B)** A CBP/MAP2 co-labeling was performed by

immunofluorescence on rat brain sections. Representative photographs of the CA1 region are shown for CBP (a), MAP2 (c) and merged (d) labelings. The total number of cells is visualized by Hoechst staining of nuclei (b). CBP is primarily expressed in pyramidal neurons as compared to other cells. Scale bar: 50 μ m.

Supplemental figure 4: HAT protein expression. (A) CBP, p300 and PCAF mRNA expression levels were evaluated by RT-qPCR in the dorsal hippocampus of control (Visible platform, VPf) and learning (Hidden platform, HPf) groups after a 1- day training period in the MWM (n=6/group). Values were normalized to the 18S ribosomal subunit and the fold inductions. Student *t*-test: *ns*: non significant. **(B)** HAT levels were assessed by western blot in nuclear protein extracts prepared from the cerebellum of control (Visible platform, VPf) and learning (Hidden platform, HPf) rat groups. Typical blots are shown in duplicates. Blots were quantified (n=7 per group) and results normalized against actin are shown (right). A student *t*-test revealed no significant difference in the amount of the different HATs between the two groups.

Supplemental figure 5: Histological verification of lesions (A), visible platform data (B) and typical swimming tracks (C) in Lesion rats. (A) Effects of intraseptal injections of 192 IgG-saporin on the optical density (OD) of AChE staining in various brain structures and on the number of ChAT- and Parv-positive neurons in the basal forebrain. Data are presented as means \pm SEM. They illustrate the effect of the double lesion on cholinergic markers in various brain structures: AChE stands for acetylcholinesterase, ChAT for choline acetyltransferase, Parv for parvalbumine, V1 and V2 for visual areas 1 and 2, respectively. The number of neurons indicated is that counted on both sides. * Significantly different from Sham, $p < 0.05$. Between brackets in the right column are the significant lesion-induced effects given in % reduction from sham values. Analysis of the ODs found in the different brain regions analyzed only revealed a significant difference in the dorsal ($F_{(1,17)} = 8,7$, $p < 0.01$) and in the ventral ($F_{(1,17)} = 6,9$, $p < 0.05$) portions of the posterior hippocampus, confirming a partial cholinergic denervation of the hippocampus. In the basal forebrain, we also found evidence for relatively selective lesions of the septal cholinergic neurons. Indeed, the number of ChAT-positive neurons was reduced by 85% and 83% in the medial septum and vertical limb of the diagonal band of Broca, respectively, and both decreases were significant ($F_{(1,19)} =$

42.7 and 9.8, respectively, $p < 0.01$). In the nucleus basalis magnocellularis (NBM), the decrease was much weaker (-31%), but reached significance ($F_{(1,19)} = 10,2$, $p < 0.01$). Concerning the number of Parv-positive neurons, we found no significant modification in the medial septum and in the NBM, but in the vertical limb of the diagonal band of Broca, the decrease (-48%) was significant ($F_{(1,19)} = 9,4$, $p < 0.01$). Thus, although the lesions did not reach an exclusively cholinergic impact, they appeared as relatively selective, both anatomically and neurochemically, as they achieved their maximal cholinergic effect in the medial septum and the vertical limb of the diagonal band of Broca. The weaker effects of 192 IgG-saporin in the NBM can be explained by diffusion of small amounts of the immunotoxin, the septum and the NBM being contiguous regions. The damage to Parv-positive neurons, when observed, is usually interpreted as a consequence on closely neighboring regions of toxic products that are released by cholinergic neurons during their 192 IgG-saporin-triggered degeneration.

(B) Water-maze performance with a visible platform during one session of 4 consecutive trials in Sham versus operated rats. Average distances (\pm SEM) to reach the platform in rats subjected to sham operations (Sham) or lesions (Lesion) showed a significant decrease over trials in both groups (two-way ANOVA: $F(3,57) = 37.11$, $p < 0.005$), although Sham rats were better than Lesion rats on the 4th trial ($p < 0.005$). In addition, the group effect showed a tendency toward significance ($F(1,19) = 4.00$, $p = 0.06$), but there was no interaction between the two factors ($F(3,57) = 1.95$, $p > 0.05$). The average performance over the 4 consecutive trials did not differ significantly between the two groups: 9.2 ± 0.5 (s.e.m) for Sham-operated versus 10.8 ± 0.7 (s.e.m) for the Lesion rats (Student's *t* test, $p=0.06$).

(C) Typical swimming tracks corresponding to retention of rats presented on figure 5B. Swimming tracks were recorded during the probe trial (performed 1hr after the last acquisition trial) in rats trained for 3 consecutive days. Rats were subjected to a sham-operation (Sham rat 1) or to a double lesion combining NMDA injections into the entorhinal cortex and 192 IgG-saporin injections into the medial septum (Lesion rat 2, Lesion rat 3). The former location of the platform is indicated by the black-filled circle in the south-east quadrant.

Supplemental figure 6: Evaluation of histone H3 and H2B acetylation levels in the cerebellum in the double lesioned rat model. Acetylated (Ac) and total (Tot)

histone levels were measured by Western blot analyses for H3 and H2B histones in total extracts obtained from the cerebellum of home cage rats (Basal conditions; Sham, n = 6; Lesion, n = 7) or of trained rats (Learning conditions: HPf group during 3 days for all rat groups; Sham, n = 7; Lesion, n = 7). Lysine acetylations measured are H3K9K14 and H2BK5K10K15K20. Typical western blots are represented in duplicates. Quantified results are represented as fold induction of the Ac/Tot ratio for each histone. The ratio obtained in the control condition is arbitrarily set at 100%. Sham, Sh; Lesion, Les. A student *t*-test revealed no significant difference between groups and conditions.